

Dynamics of a Local Algorithm for Simulating Coulomb Interactions

A. C. Maggs

Laboratoire de Physico-Chimie Théorique, ESPCI-CNRS, 10 rue Vauquelin, 75231 Paris Cedex 05, France.

(Dated: December 2, 2024)

Charged systems interacting via Coulomb forces can be efficiently simulated by introducing a local, diffusing degree of freedom for the electric field. This paper formulates the continuum electrodynamic equations corresponding to the algorithm and studies the spectrum of fluctuations when these equations are coupled to mobile charges. I compare the calculations with simulations of a charged lattice gas, and study the dynamics of charge and density fluctuations.

INTRODUCTION

Molecular dynamic simulation of charged condensed matter systems is slow and difficult [1]. In standard methods, such as optimized Ewald summation [2, 3], fast multiple methods [4, 5] or the fast Fourier transform, extensive and time consuming bookkeeping is needed because of the range of the Coulomb interaction. This bookkeeping often scales badly when implemented on modern multiprocessor machines which are used in the simulation of the largest systems. Naive Monte-Carlo methods are particularly inefficient since the motion of a single particle in an N particle simulation requires the recalculation of the Coulomb interaction with all other particles, leading to a complexity in $O(N)$ for an update in the position of a single particle

Recently, [6] a *local algorithm* with complexity scaling as $O(1)$ per update was introduced for the Monte-Carlo simulation of charged particles. In this algorithm an auxiliary electric field \mathbf{E} is coupled to the charge density. The dynamics of \mathbf{E} are chosen so that the equilibrium distribution is determined by the Coulomb interaction. Due to the locality of the algorithm the method is trivial to implement on multiprocessor machines. In this paper we study the dynamics of the algorithm in order to understand the relaxation processes and time scales involved in a typical simulation. Simulations are performed on a model of a charged lattice gas to demonstrate the diffusive propagation of charge and density fluctuations.

The algorithm is based on implementing Gauss's law

$$\text{div } \mathbf{E} = \rho/\epsilon_0 \quad (1)$$

in which ρ is the charge density and ϵ_0 the dielectric constant as an exact dynamic constraint on the Monte-Carlo algorithm.

The system is discretized by placing charged particles on the vertices of a cubic lattice, $\{i\}$. The electric field $\mathbf{E}_{i,j}$ is associated with the oriented links $\{i,j\}$ of the lattice. The simulation starts with Gauss's law satisfied as an initial condition. There are two possible Monte-Carlo moves: Firstly, fig. (1), we displace a charge, e , situated on the leftmost lattice site, A, to the rightmost site, B. The discretized constraint

$$\sum_{j,\alpha} E_{i,j}^\alpha = \rho_i/\epsilon_0 \quad (2)$$

with ρ_i the charge at the site i and where α is one of $\{x, y, z\}$ is again satisfied if the field associated with the connecting

link is updated according to the rule $E_{A,B}^x \rightarrow E_{A,B}^x - e/\epsilon_0$. Secondly we update the field configurations, fig. (2), by modifying the four field values of a single plaquette by a pure rotation; $E_{1,2}^y$ and $E_{4,1}^x$ increase by an increment Δ whereas $E_{4,3}^y$ and $E_{3,2}^x$ decrease by Δ so that at each vertex the sum of the entering and leaving fields is unchanged. The basic *dynamic* degree of freedom in the algorithm is a circulation or rotation, Θ , associated with each plaquette of the network.

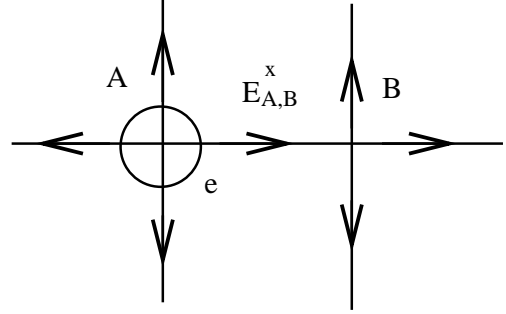


FIG. 1: Motion of a charge e from A to B is associated with a modification of the field on the connecting link: $E_{A,B}^x \rightarrow E_{A,B}^x - e/\epsilon_0$.

In the first section of the paper we formulate the continuum limit of the evolution equations and show that they lead to diffusive evolution of the electric field. We then couple the electric field to a mobile gas of charged particles and compare the solutions of the coupled plasma equations to simulations. When the algorithm is implemented as a molecular dynamics algorithm rather than a Monte-Carlo method we show that the equations are closely related to the Maxwell electromagnetic theory.

DIFFUSIVE ELECTRODYNAMICS

Fundamental equations

We start with a toy example to motivate our derivation of the effective large scale equations obeyed by the electric field: a single particle diffusing in a harmonic potential with energy $\mathcal{U} = Kx^2/2$. The equation of motion is found by taking the derivative of the energy with respect to the dynamic coordinate x and then balancing the resulting force against a relax-

ation process linear in the velocity

$$\xi \frac{dx}{dt} = -Kx + f(t) \quad (3)$$

where $f(t)$ is an external forcing term. ξ the inverse mobility sets the characteristic time scale of the relaxation of x and is a function of the step size of the Monte-Carlo trial moves. A first order (in time) algorithm, such as Monte-Carlo, for the simulation of a particle in such a potential is essentially a discretized realization of this stochastic differential equation. The Langevin description is completed by specifying f , so as to obey the fluctuation dissipation theorem. We now turn to the equations for the electric field. Firstly we examine the field in absence of current then we shall find the coupling of the field to external sources.

The discretized energy of the electric field is given by

$$\mathcal{U} = \frac{\epsilon_0}{2} \sum_{i,j} \mathbf{E}_{i,j}^2 \quad (4)$$

The basic variables in the dynamics of the field are, however, not \mathbf{E} but rather the rotational degrees of freedom which are updated independently at each time step. The conjugate force acting on this variable is a torque. We define on each plaquette in the $\{x, y\}$ plane the angular variable Θ^z . We group the angle corresponding to the three possible plaquette orientations into a vector Θ . The physical field \mathbf{E} is sensitive to derivatives of Θ : Studying fig. (2) one sees that $E_{1,2}^y$ is given by the x variation of the z component of Θ . This we recognize as part of the curl operator acting on the field Θ . The complete relation between a local variation in \mathbf{E} and a local variation in Θ is thus

$$\delta \mathbf{E} = \text{curl } \delta \Theta \quad (5)$$

where in the discretized model derivatives are to be understood as finite differences with \mathbf{E} living on links and Θ on plaquettes.

Modification of the circulation Θ_A^z in fig. (2) by Δ gives rise to a new contribution to the energy of the plaquette.

$$\bar{\mathcal{U}} = \frac{\epsilon_0}{2} \left((E_{4,1}^x + \Delta)^2 + (E_{1,2}^y + \Delta)^2 + (E_{4,3}^y - \Delta)^2 + (E_{3,2}^x - \Delta)^2 \right) \quad (6)$$

Taking the derivative with respect to Δ we find a torque, \mathbf{C} , acting on the circulatory degree of freedom which is a discretized version of the curl of the field.

$$C_z = -\frac{\partial \bar{\mathcal{U}}}{\partial \Delta} = -\epsilon_0 \left((E_{4,1}^x - E_{3,2}^x) + (E_{1,2}^y - E_{4,3}^y) \right) \quad (7)$$

$$= -\epsilon_0 \left(\frac{\partial E^y}{\partial x} - \frac{\partial E^x}{\partial y} \right) \quad (8)$$

$$= -\epsilon_0 \hat{\mathbf{k}} \cdot \text{curl } \mathbf{E} \quad (9)$$

Again the three components of the torque live on the plaquettes together with the angle Θ . By analogy with eq. (3) the evolution equation for the angle Θ is

$$\xi \frac{d\Theta}{dt} = \mathbf{C} \quad (10)$$

linking a velocity to the conjugate force. Eventually a stochastic force should also be added into this equation but we shall not need it in what follows and will thus ignore it from now on.

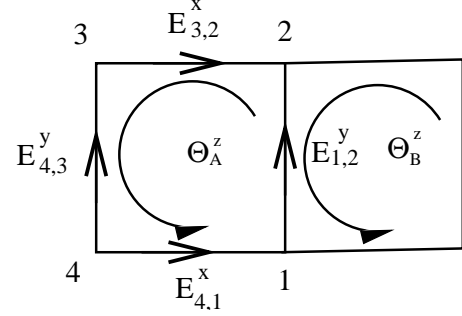


FIG. 2: Modification of the angle Θ_A^z leads to modified values of the field between on the links $\{1, 2\}$, $\{3, 2\}$, $\{4, 3\}$, $\{4, 1\}$. The field in the y direction associated with the link $E_{1,2}^y$ is given by the difference of the angles associated with the two plaquettes, Θ_A^z and Θ_B^z , which are aligned in the x direction.

Consider now the evolution of the field in the presence of a current. Take a network in which charges are present at every vertex and displace every charge to the right as in fig. (1). Then every bond in the x direction is modified by $-e/\epsilon_0$ where e is the charge displaced even though the local charge density is unchanged. If we displace the charges at a constant rate we have the evolution of the field due to the source as

$$\frac{\partial \mathbf{E}_{\text{source}}}{\partial t} = -\mathbf{J}/\epsilon_0 \quad (11)$$

Combining eqs. (5,9,10,11) we find

$$\frac{\partial \mathbf{E}}{\partial t} = (\epsilon_0 \nabla^2 \mathbf{E} - \text{grad } \rho) / \xi - \mathbf{J}/\epsilon_0 \quad (12)$$

where we have used the standard identity $\text{curl curl } \mathbf{E} = (\text{grad div } \mathbf{E} - \nabla^2 \mathbf{E})$ and Gauss's law. Equation (12) is the main result of this section giving a diffusive propagation law of the electric field in absence of external charges and currents.

In the static limit both the current and the time derivative of eq. (12) vanish. We find the same equation for the electric field

$$\nabla^2 \mathbf{E} = \text{grad } \frac{\rho}{\epsilon_0} \quad (13)$$

as is found by applying the operator $(-\text{grad})$ to the Poisson equation in conventional electrostatics. When we take the divergence of eq. (12) we discover that

$$\left(\frac{\partial}{\partial t} - \frac{\epsilon_0}{\xi} \nabla^2 \right) (\text{div } \mathbf{E} - \rho/\epsilon_0) = 0 \quad (14)$$

Again we see that Gauss's law is implemented in the method as an initial condition.

Phenomenological Dynamics of a Two Component Plasma

In this section we couple the diffusive evolution equation for the electric field eq. (12) to those of a two component plasma and study the relaxation phenomena and time scales that are to be expected when using the algorithm to simulate dense charged systems.

The equations of conservation and linear response give the following equations for the charge degrees of freedom:

$$\begin{aligned}\frac{\partial c^+}{\partial t} &= -\text{div } \mathbf{J}^+ \\ \frac{\partial c^-}{\partial t} &= -\text{div } \mathbf{J}^- \\ \mathbf{J}^+ &= -D \text{grad } c^+ + e\mu c^+ \mathbf{E} \\ \mathbf{J}^- &= -D \text{grad } c^- - e\mu c^- \mathbf{E}\end{aligned}\quad (15)$$

Where c^+ and c^- are the number density of the positive and negative charges, $\pm e$. \mathbf{J}^\pm are the number current density. From these equations we find the equations obeyed by the total density c and the charge density ρ . We note that the diffusion coefficient D and the mobility, μ are linked by the Einstein relation $D = k_B T \mu$.

Taking the sum and difference of the equations (15) we find

$$\begin{aligned}\frac{\partial c}{\partial t} &= D \nabla^2 c \\ \frac{\partial \rho}{\partial t} &= -\text{div } \mathbf{J} \\ \mathbf{J} &= e^2 \mu c_0 \mathbf{E} - D \text{grad } \rho - \mu \text{grad } \phi_e(t)\end{aligned}\quad (16)$$

where we have linearized the equations about a mean density c_0 . $\mathbf{J} = e\mathbf{J}^+ - e\mathbf{J}^-$ is the electric current density. $\phi_e(t)$ is an externally imposed potential that we shall use to calculate charge-charge correlation functions. Substituting eq. (16) for \mathbf{J} in (12) we find

$$\begin{aligned}\frac{\partial \mathbf{E}}{\partial t} &= \epsilon_0 / \xi \nabla^2 \mathbf{E} - e^2 \mu c_0 / \epsilon_0 \mathbf{E} \\ &+ (D / \epsilon_0 - 1 / \xi) \text{grad } \rho + \mu / \epsilon_0 \text{grad } \phi_e\end{aligned}\quad (17)$$

We analyze this equation by treating separately the longitudinal and transverse fluctuations. Take the curl of eq. (17) to find that the transverse components of \mathbf{E} decouple from the charge density. In Fourier space we find the dispersion law

$$(i\omega + \epsilon_0 / \xi q^2 + e^2 \mu c_0 / \epsilon_0) \mathbf{q} \wedge \mathbf{E} = 0 \quad (18)$$

In the absence of charges the mode is diffusive but the presence of a finite charge density gives a gap in the spectrum.

Consider now the equations for the charge eq. (16): With the help of Gauss's law one replaces the divergence of the field by the charge to find

$$\left(\frac{\partial}{\partial t} - D \nabla^2 + e^2 \mu c_0 / \epsilon_0 \right) \rho = -\mu \nabla^2 \phi_e \quad (19)$$

which also applies to the longitudinal mode of the electric field

$$(i\omega + Dq^2 + e^2 \mu c_0 / \epsilon_0) \mathbf{q} \cdot \mathbf{E} = \epsilon_0 \mu q^2 \phi_e \quad (20)$$

Again the spectrum has a gap at $q \rightarrow 0$.

NUMERICAL RESULTS

Dynamics

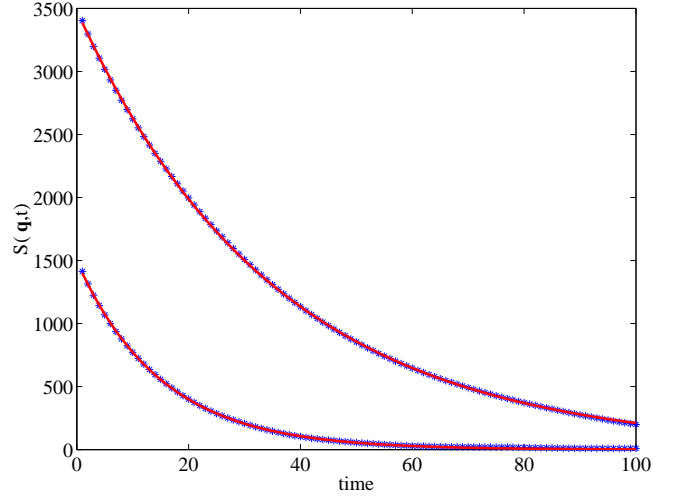


FIG. 3: Fit of a density-density, top, and a charge-charge, bottom, correlation functions eq. (22) to a single exponential. 5000 particles, network of $25 \times 25 \times 25$, mode $\mathbf{q} = 2\pi \times (2, 2, 0)$. Arbitrary units

We performed simulations of a charged lattice gas to study the dynamics of the density and charge fluctuations. Equal numbers of positively and negatively charged particles were placed on the vertices of a network which was simulated by the algorithm of [6] in a uniform dielectric background. During the simulations we measured the Fourier transform of the particle distributions

$$s(\mathbf{q}, t) = \frac{1}{\sqrt{N}} \sum_i e_i \exp(i\mathbf{r}_i(t) \cdot \mathbf{q}_i) \quad (21)$$

where the weight e_i is the charge for the charge correlation function and is unity for the density correlation function. We use this information to construct the dynamic structure factor

$$S(\mathbf{q}, t) = \langle s(\mathbf{q}, t) s(-\mathbf{q}, 0) \rangle \quad (22)$$

The result is fitted with an exponential and the decay rate plotted as a function of q^2 in figs. (3,4). The density-density correlation function displays simple diffusive behavior. The charge-charge correlation function is characterized by a gap at $q = 0$.

What do these dispersion relations imply for the equilibration of a system of charged particles? The propagation of a

signal in a dispersive medium is given by the group velocity $v_g = d\omega/dq$. Thus both the mass and charge degrees of freedom are diffusive. A simulation equilibrates in a time which scales quadratically with the linear dimensions of the system.

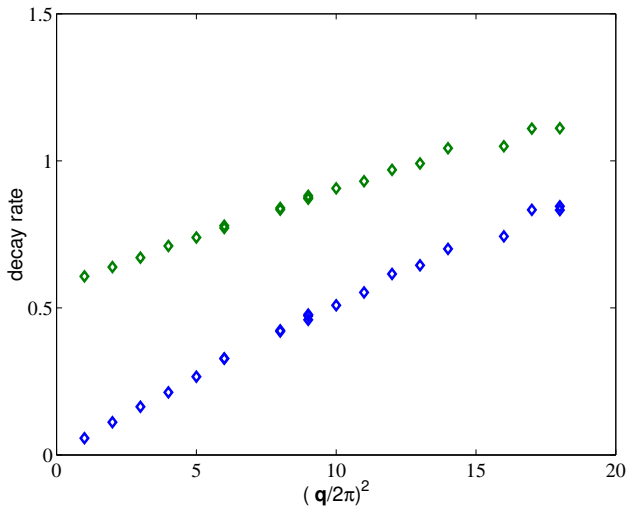


FIG. 4: Characteristic time extracted from $S(q, t)$ as a function of q^2 . Bottom curve : Density-density correlations: the mode is diffusive, eq.(16). Top curve: The charge-charge correlation function has a gap in agreement with eq. (19). Selected modes between $(q/2\pi)^2 = 1$, $\mathbf{q} = 2\pi \times (1, 0, 0)$ and $(q/2\pi)^2 = 18$, $\mathbf{q} = 2\pi \times (4, 1, 1)$. 1000 Particles, $18 \times 18 \times 18$ mesh. Vertical axis in arbitrary units.

Note that the parameters used in the derivation of the plasma dynamics are already at a coarse grained level of description: While the eq. (12) is in some sense fundamental, containing within it the exact statement of Coulomb's law and Boltzmann statistics, the eqns (16) are purely phenomenological. An example is the mobility of a particle μ which in the above theoretical presentation appears independent of the field parameters ϵ_0 and ξ . However consider the case of a charged particle pulled by an external non-electric force in the presence of a electric field which relaxes very slowly. As the particle moves it leaves behind it a "string" of electric field due the dynamics of fig. (1). This creates a back force on the particle which reduces its mobility. Monte-Carlo moves on the field spread this string over many lattice sites increasing the mobility of a charged particle. Thus the mobility of the charged particles increases when the field relaxes more rapidly.

This effect is an explanation of the curves of fig. (4) Despite the predictions of eqs. (16,19) the slope of the charge-charge and the density-density curves are slightly different; the effective diffusion coefficient of the charge fluctuations is lower than that of the density fluctuations. Slow relaxation of the electric degrees of freedom should hinder the motion of a single charged particle more than a strongly coupled, neutral pair moving in the same direction.

Screening

From the Poisson-Boltzmann equation it is known that charged systems screen. We derive this result from our dynamic equations as follows: Consider eq. (19) for the charge density in the presence of a static external potential $\phi_e(\mathbf{q})$.

$$\rho(\mathbf{q}) = \frac{q^2}{q^2 + e^2 c_0 / \epsilon_0 k_B T} \frac{\phi_e}{k_B T} \quad (23)$$

from linear response theory the structure factor is

$$S(q) = \frac{q^2}{\kappa^2 + q^2} \quad (24)$$

where the Debye length is given by $\kappa^{-2} = e^2 c_0 / \epsilon_0 k_B T$. This prediction is checked in our code by plotting $1/S(q)$ as a function of $1/q^2$, fig. (5).

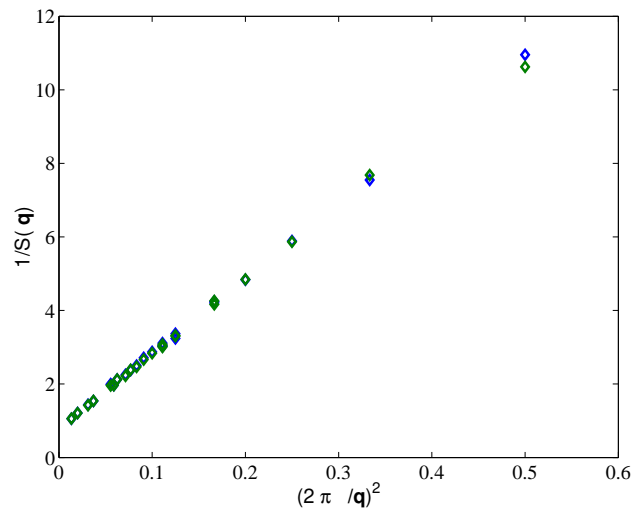


FIG. 5: Plot of $1/S(q)$ as a function of $(2\pi/q)^2$. The plot is linear as implied by eq. (24). Selected modes between $2\pi \times (1, 1, 0)$ out to $2\pi \times (5, 5, 5)$. The plasma screens interactions exponentially. 5000 charges on a network of $25 \times 25 \times 25$

Fig. (5) should be taken as very strong evidence that our algorithm is behaving correctly. It reproduces one of the most striking features of charged systems, the exponential decay of the charge-charge correlation function due to Debye screening.

Numerical Stability

In the simulations that we performed to study the dynamic and screening properties of the algorithm we were agreeably surprised by the numerical stability of the algorithm: At each update one makes an error e_p comparable to the round off error of the computer. Over many time steps this accumulates so that Gauss's law is violated. We feared that this local error would rapidly become important.

The slow propagation (in time) of numerical errors can be understood by consideration of eq. (14). Local fluctuations in the constraint $\text{div } \mathbf{E} - \rho/\epsilon_0 = 0$ spread out via a diffusion process. Since both positive and negative errors are made during a simulation there is a large degree of cancellation occurring. After a single Monte-Carlo sweep of the system Gauss's law is violated by $O(e_p)$ at each lattice site. However averaged over a sample with L^3 sites the average error per site is $O(e_p/L^{3/2})$. When simulated for $O(L^2)$ sweeps the system comes to equilibrium under the diffusive propagation of the charge and density fluctuations, we find errors of only $O(e_p/L^{1/2})$ per site. The high statistics curves of this paper were generated by using runs of length 5000 times the equilibration time. Even here the errors remained acceptably small. For even longer runs one can perform a very small rescaling of the fields to reimpose the constraint.

MOLECULAR DYNAMICS

In eq. (12) we gave the equations of motion for the electric field obeyed in the continuum limit of a Monte-Carlo simulation. In this section we shall see how local imposition of Gauss's law can be used to find a molecular dynamics algorithm for the evolution of the electric field. We continue to describe the basic dynamic degree of freedom as an angular variable, Θ , which is linked to the electric field by eq. (5). This variable is associated with a conjugate angular momentum, \mathbf{p}_θ and moment of inertia I_θ , in order to give the equations of motion of the field the usual Hamiltonian structure. The resulting second order equations will display propagating, wave like features rather than the diffusive propagation characteristic of eq. (12). We now give equations for the molecular dynamics simulation of a charged system in which the charges are interpolated onto a mesh, in a manner similar to P^3M simulations [7].

The charge of a particle contained within a cube of the network is firstly interpolated to the corners of the cube. As the particle moves the electric field which is defined on the 12 links defining the cube is updated by an amount proportional to the charge transfer between the corners of the cube, exactly as in fig. (1). Each link field $\mathbf{E}_{i,j}$ is the result of the rotation of a variable Θ defined on the faces of the cube rotating at angular velocity $\mathbf{p}_\theta/I_\theta$. As above the torque on the rotational degree of freedom of a plaquette is given by $\mathbf{C} = -\epsilon_0 \text{curl } \mathbf{E}$. Using eq. (5,11) we find the following equations obeyed by the fields:

$$\begin{aligned} \frac{\partial \mathbf{p}_\theta}{\partial t} &= -\epsilon_0 \text{curl } \mathbf{E} \\ \frac{\partial \mathbf{E}}{\partial t} &= \frac{1}{I_\theta} \text{curl } \mathbf{p}_\theta - \mathbf{J}/\epsilon_0 \\ \text{div } \mathbf{E} &= \rho/\epsilon_0 \end{aligned} \quad (25)$$

where the differential operators are to be interpreted as the appropriate difference when acting on the lattice variables.

The equations (25) are the Maxwell equations with \mathbf{p}_θ playing the role of the magnetic field \mathbf{B} . Their derivation shows that \mathbf{p}_θ is a momentum variable which can be coupled to a thermostat order to ensure equilibration of the field degrees of freedom [8]; the linear equations that we have found for the electric field are likely to equilibrate rather slowly and should be coupled to an explicit heat bath so that the equation for \mathbf{p}_θ becomes

$$\frac{\partial \mathbf{p}_\theta}{\partial t} = -\epsilon_0 \text{curl } \mathbf{E} - \gamma \mathbf{p}_\theta + \zeta(t) \quad (26)$$

where γ is a weak damping coefficient and $\zeta(t)$ a Langevin noise. Taking the divergence of eq. (26) we find that the fourth Maxwell equation, $\text{div } \mathbf{p}_\theta = 0$, is violated by the noise in the equations.

The particles in the simulation are coupled to the electric field:

$$\begin{aligned} \frac{\partial \mathbf{p}_i}{\partial t} &= e_i \mathbf{E}(\mathbf{r}_i) \\ \frac{\partial \mathbf{r}_i}{\partial t} &= \mathbf{p}_i/m_i \end{aligned} \quad (27)$$

With \mathbf{r}_i , \mathbf{p}_i and m_i the positions, momenta and masses of the i 'th particle. One would also add in the other, non Coulombic forces on the particles to these equations of motion and couple the momentum variable to a heat bath. We construct the following functional using the equations of motion eq. (25,27)

$$\dot{\mathcal{H}} = \sum_i \frac{\mathbf{p}_i}{m_i} \cdot \frac{\partial \mathbf{p}_i}{\partial t} + \int \left(\epsilon_0 \mathbf{E} \cdot \frac{\partial \mathbf{E}}{\partial t} + \frac{\mathbf{p}_\theta}{I_\theta} \cdot \frac{\partial \mathbf{p}_\theta}{\partial t} \right) d^3\mathbf{r} \quad (28)$$

and make use of the identity

$$\text{div} (\mathbf{p}_\theta \wedge \mathbf{E}) = \mathbf{E} \cdot \text{curl } \mathbf{p}_\theta - \mathbf{p}_\theta \cdot \text{curl } \mathbf{E} \quad (29)$$

to transform the volume integral in eq. (28) to a surface integral.

$$\dot{\mathcal{H}} = \frac{\epsilon_0}{I_\theta} \int \mathbf{p}_\theta \wedge \mathbf{E} \cdot d\mathbf{S} \quad (30)$$

The integrand is the Poynting vector [9]. For periodic boundary conditions the integral vanishes and we find that

$$\mathcal{H} = \sum_i \frac{\mathbf{p}_i^2}{2m_i} + \int \left(\epsilon_0 \frac{\mathbf{E}^2}{2} + \frac{\mathbf{p}_\theta^2}{2I_\theta} \right) d^3\mathbf{r} \quad (31)$$

is a constant of the motion. This the total energy of the system.

The partition function is calculated from

$$\mathcal{Z} = \int \mathcal{D}\mathbf{p}_i \mathcal{D}\mathbf{p}_\theta \int \mathcal{D}\mathbf{r}_i \int \mathcal{D}\mathbf{E} e^{-\beta\mathcal{H}} \quad (32)$$

The integration region is the set of configurations available to the equations of motion. Integration over the momenta is easy to perform in the presence of Langevin noise acting on momenta which destroys the constraints and conservation laws associated with the variable \mathbf{p}_θ in Maxwell's equations. What

remains is the integral over the electric fields and particle positions. If the dynamics were ergodic we would integrate over all values of the field. However Maxwell's equations, even in the presence of noise on the momentum degree of freedom, include Gauss's law. This constrains the electric field and the partition function is given by

$$Z_c = \int e^{-\beta V} \mathcal{D}\mathbf{r}_i \int \mathcal{D}\mathbf{E} e^{-\int \frac{\beta \mathbf{E}^2}{2} d^3\mathbf{r}} \prod_{\mathbf{r}} \delta(\text{div } \mathbf{E} - \rho/\epsilon_0) \quad (33)$$

where, now, all degrees of freedom are freely integrated over. V is the potential coming from the non-Coulombic interactions. As shown in [6] it is this constrained configurational integral that leads to effective Coulomb interactions. It is important to note that the equations of motion (27) for the particles do not contain the Lorentz force.

The above reasoning was performed on the continuum limit of the evolution equations, however, one can perform the arguments with the discretized equations for the field and one finds an equivalent result for the conservation of energy, and a similar constrained partition function. One must simply make sure that the electric force on the particles $e_i \mathbf{E}(\mathbf{r}_i)$ in eq. (27) and the current, \mathbf{J} , in eq. (25) are self consistently discretized so that when building the functional eq. (28) these two terms cancel.

We find rather remarkable results: We can simulate a model with a circulatory degree of freedom on each plaquette with dynamics such that the *equilibrium* distribution function generated by the system is that of a charged system with Coulomb interactions. The continuum limit of the equations describing the system are very close to Maxwell's equations for electromagnetism with the magnetic field playing the role of an angular momentum defined at the level of the plaquettes. The velocity of propagation of waves can be freely varied by modifying the moment of inertia of the rotational mode. By construction the thermodynamics are unchanged by this modification so that the propagation velocity can be used as an optimization parameter in the simulation. Proper equilibration to the Boltzmann distribution is ensured by modification of one of the Maxwell equations eq. (26) which leads to violations of the equation $\text{div } \mathbf{B} = 0$.

Finally our law for the *local* update of the electric field after movement of a particle, fig(1), is a discretized version of

the Maxwell displacement current. Almost all of the structure of Maxwell's equations is derived from the local constraint of Gauss's law plus Hamiltonian structure on the field equations. Due to the underlying lattice the equations are *not* relativistically invariant. There is a very definite, preferred frame of reference where the lattice is stationary. Maxwell's equations only appear in this reference frame.

CONCLUSIONS

We have analyzed a Monte-Carlo algorithm for the simulation of long range Coulomb interactions. We have seen that propagation of the electric degrees of freedom is diffusive, however by construction the dynamics sample the equilibrium Boltzmann distribution of the charged system. The locality of the algorithm allow fast and *simple* implementations even on multiprocessor computers with high communication overheads. The method is easily adapted to a molecular dynamics treatment. The dynamics of the field are then almost Maxwellian. However one should couple the momentum variable to an external reservoir to ensure that the linear degrees of freedom of the electric field truly sample the full phase space. We have verified that the Monte-Carlo algorithm reproduces well known features of the two component plasma such as screening.

-
- [1] T. Schlick, R. D. Skeel, A. T. Brunger, L. V. Kal, J. A. Board, J. Hermans, and K. Schulten, *J. Comp. Phys.* **151**, 1617 (1998).
 - [2] J. V. L. Beckers, C. P. Lowe, and S. W. de Leeuw, *Molecular Simulation* **20**, 269 (1988).
 - [3] J. W. Perram, H. G. Petersen, and S. W. de Leeuw, *Molecular Phys.* **65**, 875 (1988).
 - [4] J. E. Barnes and P. Hut, *Nature* **324**, 446 (1986).
 - [5] L. Greengard and V. Rokhlin, *J. Comput. Phys.* **73**, 325 (1987).
 - [6] A. C. Maggs and V. Rossetto, *cond-mat/0111009* (2001).
 - [7] R. W. Hockney and J. W. Eastwood, *Computer Simulation using Particles* (Adam Hilger, 1988).
 - [8] D. Frenkel and B. Smit, *Understanding Molecular Simulation* (Academic Press Limited, London, 1996).
 - [9] J. D. Jackson, *Classical Electrodynamics* (Wiley, 1999).